JOURNAL OF BACTERIOLOGY, Nov. 1991, p. 7395–7400
0021-9193/91/227395-06$02.00/0

Vol. 173, No. 22

Absence of *hisT*-Mediated tRNA Pseudouridylation Results in a Uracil Requirement That Interferes with *Escherichia coli* K-12 Cell Division

HO-CHING TIFFANY TSUI,[1] PEGGY J. ARPS,[2]† DENNIS M. CONNOLLY,[2] AND MALCOLM E. WINKLER[1]*

Department of Microbiology and Molecular Genetics, University of Texas Medical School, Houston, Texas 77030,[1] and Department of Molecular Biology, Northwestern University Medical School, Chicago, Illinois 60611[2]

Received 13 May 1991/Accepted 16 September 1991

We show that *hisT* function is required for normal growth of *Escherichia coli* K-12, since a lack of *hisT*-mediated pseudouridine tRNA modification causes a uracil requirement that interferes with cell division. We also show that *hisT* transcription is positively growth rate regulated in exponentially growing bacteria and is induced during the transition from exponential to stationary growth phase.

Previous studies have concluded that pseudouridine modifications in the anticodon stem and loop of tRNA molecules are dispensable for cellular growth (7, 9, 10). It was also suggested that the *hisT* gene, which encodes pseudouridine synthase I (PSUI), which catalyzes pseudouridylation in anticodon stems and loops, is constitutively expressed in bacteria (1, 7). However, both these conclusions were based on a limited number of experiments with unspecified *hisT* mutants that might have retained residual activity (e.g., see reference 9). Unexpectedly, we (and others who requested strains) observed severely limited growth of *hisT* chromosomal insertion mutants in minimal medium, which caused us to reexamine the issues of *hisT* requirement and regulation.

***hisT* insertions result in a uracil requirement that interferes with cell division.** *hisT*::Km^r knockout mutants (Fig. 1) (4) exhibited a substantially longer lag period than their isogenic parents when they were downshifted from Luria-Bertani medium plus 30 μg of cysteine per ml (LBC) to minimal (E) salts–0.4% glucose–0.01 mM $FeSO_4$ (MMG) (Table 1). After lagging, the *hisT*::Km^r mutants eventually resumed exponential growth but at a much lower rate than reported previously for *hisT* mutants of *Escherichia coli* and *Salmonella typhimurium* (see below) (9, 10). Several controls confirmed that the long lag period and slow growth were due to a lack of *hisT* function rather than polarity in the complex *pdxB-hisT* operon (Fig. 1) (2–4, 18, 21). The experiment was repeated with two common prototrophic *E. coli* K-12 genetic backgrounds, W3110 (strains NU814 and NU426) and MG1655, with similar results (Table 1). Recombinant plasmids that contain *hisT*$^+$ but lack downstream genes in the operon (2, 18) fully complemented the *hisT*::Km^r phenotype by restoring the lag period and growth rate to that of the parent strain (strains NU660 and NU654, Table 1). Finally, the extremely low growth rate, but not the long lag period, was specific to a lack of *hisT*-mediated pseudouridine tRNA modifications and was not a general property of mutants deficient in other tRNA modifications. For example, *miaA* mutants, which lack the ms^{2}i^{6}A-37 [2-methylthio-N^6-(Δ^2-isopentenyl)-adenosine at position 37] tRNA modification (11), also experienced substantial difficulty in recovering from nutrient downshifts but grew only 10 to 20% more

TABLE 1. Increased lag time, doubling time, and filament formation of *hisT*::Km^r insertion mutants[a]

Strain[b]	Lag time (min)	Doubling time (min)	Observed filament formation[c]
NU426 (parent)	321 ± 29	71 ± 0.5	−
NU610 (*hisT*::Km^r − 1)	511 ± 19	215 ± 54	++++
NU611 (*hisT*::Km^r − 2)	473 ± 48	312 ± 37	++++
NU743 (*miaA*::Km^r − 1)	420 ± 0	93 ± 2	−
NU612 (*dsg-1*::Km^r)	ND	ND	−
NU607 (*asd'*::Km^r)	ND	ND	++++
NU660 [NU610(ψ300)][d]	328 ± 26	76 ± 1	−
NU654 [NU607(pNU61)][e]	340 ± 20	73 ± 4.5	−
NU814 (parent)	378 ± 7.2	95 ± 3.6	−
NU1687 (*hisT*::Km^r − 1)	555 ± 30	265 ± 70	++++
NU1688 (*miaA*::Km^r − 1)	550 ± 40	105 ± 7	−
MG1655 (parent)	260 ± 25	94 ± 1	−
NU1689 (*hisT*::Km^r − 1)	354 ± 22	223 ± 17	++++

[a] Overnight cultures (5 ml) grown in LBC medium at 37°C were collected by low-speed centrifugation, washed with 15 ml of Vogel-Bonner minimal (E) salts (12), and resuspended in 2 ml of MMG. A 0.1-ml volume of resuspended cells was inoculated into 10 ml of MMG in Nephlo flasks, which were shaken vigorously at 37°C. Culture growth was monitored by using a Klett colorimeter at 660 nm, and cell shape was observed with a phase-contrast microscope (see Fig. 1). Values are expressed as means ± standard errors of the means and were obtained from two separate experiments. ND, not determined.

[b] NU426, a W3110 *sup*(Am) prototroph, and NU814, a W3110 *tna-2 sup*^{0} prototroph, were originally obtained from C. Yanofsky, and the MG1655 prototroph was obtained from C. Gross. The *hisT*::Km^r − 1 and *hisT*::Km^r − 2 alleles contain the kanamycin resistance cassette in opposite orientations (Fig. 1) (4). The *hisT*::Km^r − 1 (4) and *miaA*::Km^r − 1 (11) insertion mutations were moved from strains NU610 and NU743 into strains NU814 and MG1655, respectively, by standard generalized transduction (12) with the P1*kc* or P1*vir* phage.

[c] −, no filaments seen; ++++, filaments predominant, with very few single cells.

[d] ψ300, *asd'*$^+$ *hisT*$^+$ plasmid (18).

[e] pNU61, *asd'* mutant *hisT*$^+$ plasmid (2).

* Corresponding author.

† Present address: Institute of Arctic Biology, University of Alaska, Fairbanks, AK 99775.

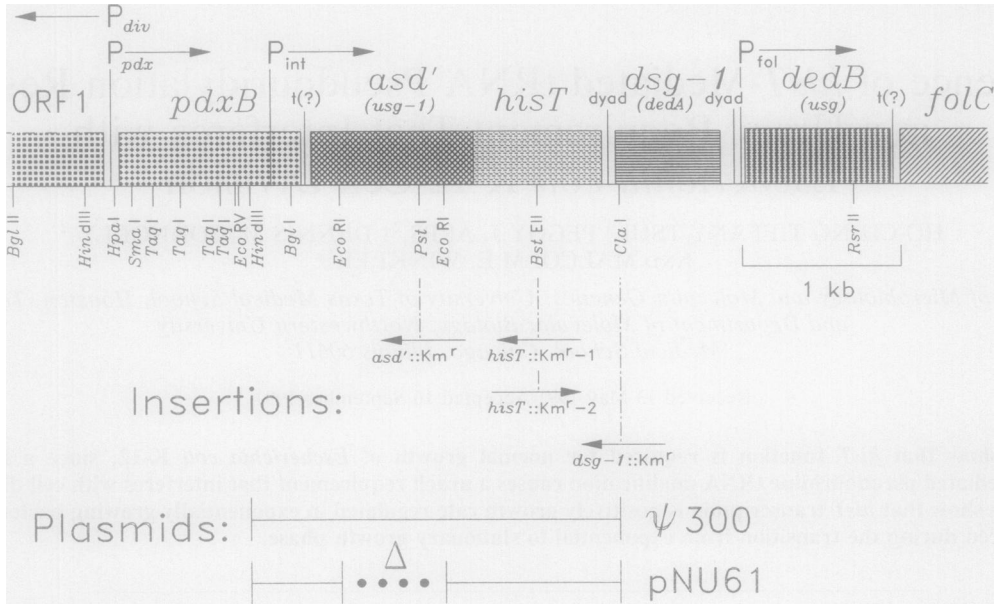

FIG. 1. Structure of the complex *pdxB-hisT* operon and locations of chromosomal kanamycin resistance cassette (Km^r) insertion mutations used in this study. Fragments of chromosomal DNA contained in recombinant plasmids ψ300 and pNU61 are also indicated. The *pdxB-hisT* operon consists of at least four genes: *pdxB* (probably erythronate-phosphate dehydrogenase), *asd'* (evolutionarily related to aspartate semialdehyde dehydrogenase), *hisT* (tRNA PSUI), and *dsg-1* (downstream gene from *hisT* of unknown function) (see references in reference 21). Alternative gene designations are given in smaller letters below the preferred names. It is presently unclear whether *dedB* and *folC* are additional downstream genes in the operon (21). *hisT* is transcribed from at least two promoters (P_{pdx} and P_{int}) (2, 4), and P_{pdx} overlaps a divergent promoter (P_{div}) of approximately equal strength under some culture conditions (21). Regions of strong intercistronic dyad symmetry or that possibly serve as rho-independent transcription terminators are indicated (dyad and t(?), respectively). Construction of chromosomal insertion mutations and recombinant plasmids ψ300 and pNU61 are described in references 4 and 2 and 18, respectively.

slowly than the $miaA^+$ parent in MMG (Table 1, strains NU1688 and NU743).

To understand the severe growth defect exhibited by *hisT* mutants in minimal medium, we examined cells stained with DAPI (4′,6-diamidino-2-phenylindole) by using combined phase-contrast and fluorescence light microscopy (Fig. 2) (15). The $hisT^+$ parent and the *hisT*::Km^r mutant formed normal-appearing, separated cells in MMG and LBC medium, respectively (Fig. 2a and b). By contrast, *hisT*::Km^r mutants in MMG exhibited a strong defect in cell division that resulted in filament formation (Fig. 2d and e). The combined optics revealed that the *hisT* mutants were defective in nucleoid segregation, septum formation, and cell separation, and their cell volumes were altered. Again, filament formation by *hisT* mutants was found for both genetic backgrounds and was complemented by the $hisT^+$ gene (Table 1). Consistent with the lack of a polarity effect, an insertion in *dsg-1*, which is immediately downstream from *hisT* and encodes a hydrophobic protein that fractionates with the inner membrane (Fig. 1) (4, 5), resulted in a failure to form filaments (strain NU612, Table 1). By contrast, an insertion in upstream gene *asd'*, which appears to be translationally coupled to and thereby required for *hisT* expression (Fig. 1) (18), again resulted in filament formation (strain NU607, Table 1). Previously, filament formation had been noted for *S. typhimurium hisT* mutants in media containing high concentrations of carbon sources (2%) and at temperatures greater than 37°C (19). By contrast, we observed filament formation by *hisT* mutants at 30 to 42°C in minimal medium supplemented with low (0.15%) glucose or moderate (0.6%) glycerol concentrations (data not shown).

Bruni et al. (9) reported earlier that the *hisT105* allele, which appears to be somewhat leaky, inhibits *E. coli* growth, but not nearly to the extent shown in Table 1 (127 versus >215 min). They also reported that the growth of the *hisT105* mutant could be restored to that of the $hisT^+$ parent by the addition of 0.71 mM uracil, 0.5 mM methionine and isoleucine, 0.03 mM thiamine, 0.049 mM pyridoxine, and 0.4 mM adenine to MMG (9). We found that of these six compounds, when tested together and separately (Table 2), uracil alone

FIG. 2. Filamentous phenotype of *hisT*::Km^r mutants and reversal by uracil addition. Bacteria were grown to stationary phase at 37°C in the media indicated below before samples were prepared for microscopy. Cells were stained with DAPI to show nucleoids as detailed in reference 15. Panels a, b, c, and e are combined fluorescence and phase-contrast images, and panel d is a phase-contrast image only. NU426 ($hisT^+$) parent in MMG (a) and NU610 (*hisT*::Km^r) in LBC (b) show normal, separated cells. NU610 in MMG plus 0.71 mM uracil (c) shows cells with 2- to 4-μm lengths, which is about twice that of NU426 (see panel a) but much shorter than the lengths of cells of NU610 cultures lacking uracil (see panels d and e). Long (50-μm) filaments were absent, although short (<10-μm) filaments were occasionally seen. NU610 in MMG without uracil (d and e) showed extremely long filaments made up of segments that appeared to contain separated septa but that were still connected to each other via extracellular material (see panel d). Individual segments were much longer than separated, normal cells (2 to 6 versus 1 to 2 μm [see panels a and b]). Many small nucleoids were found in each segment, and long unseparated nucleoids were also seen in some cells (e). The filamentous phenotype was largely reversed by addition of 0.71 mM uracil (see c). Scale bar = 10 μm.

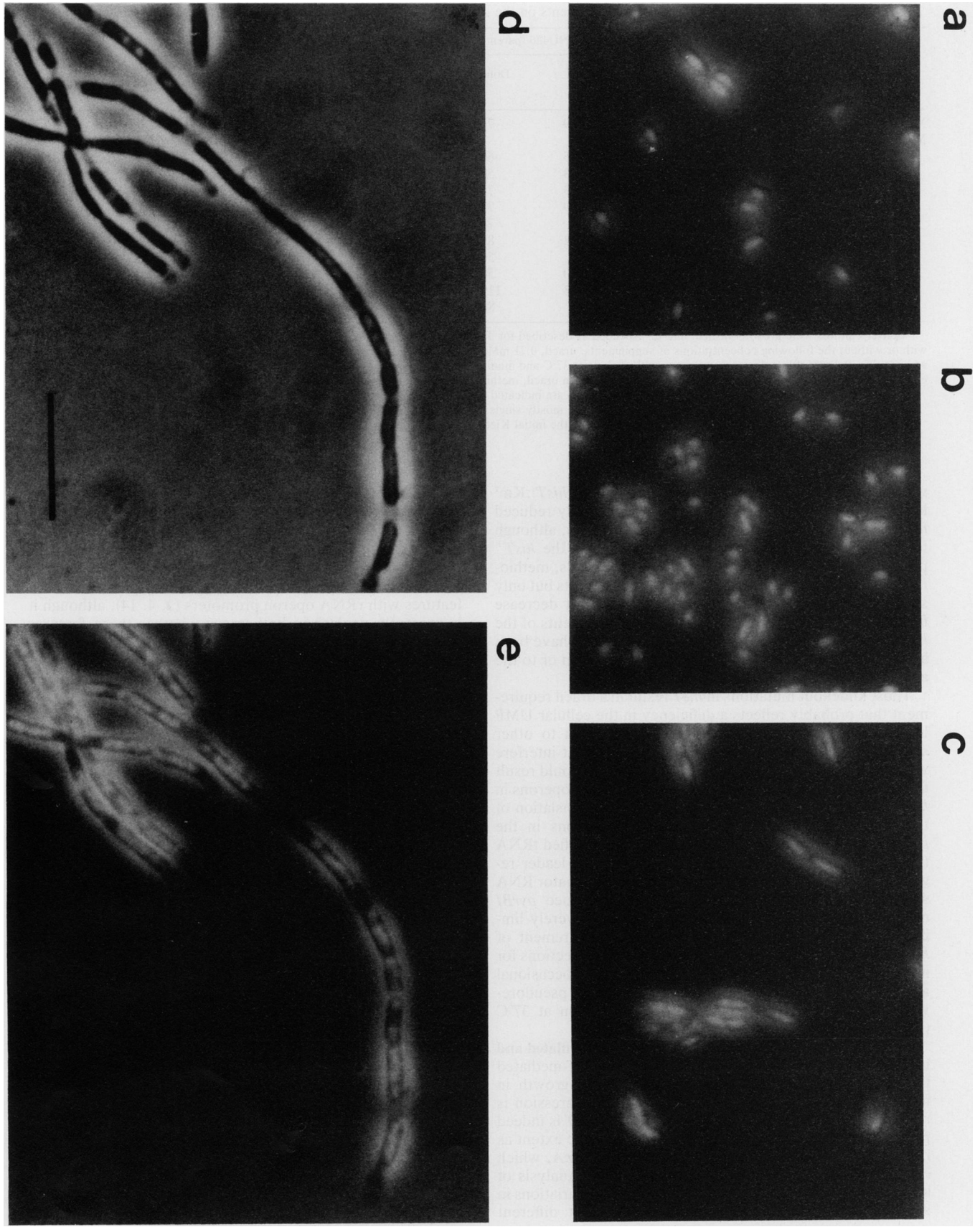
a
b
c
d
e

TABLE 2. Effects of different supplements on the lag and doubling times of a *hisT*::Km^r insertion mutant[a]

Medium	NU426 (parent)		NU610 (*hisT*::Km^r)		
	Lag time (min)	Doubling time (min)	Lag time (min)[b]	Doubling time (min)[b]	Observed filament formation[c]
MMG alone	321 ± 29	71 ± 0.5	511 ± 19 (159)	215 ± 54 (303)	++++
MMG plus:					
Uracil	314 ± 25	60 ± 1.8	420 ± 18 (134)	80 ± 4.7 (133)	+
Methionine	236 ± 33	59 ± 2.4	292 ± 42 (123)	158 ± 4.3 (268)	++++
Isoleucine	266 ± 23	71 ± 2.4	428 ± 52 (161)	223 ± 23 (328)	++++
Thiamine	321 ± 29	73 ± 2	511 ± 19 (159)	278 ± 68 (380)	++++
Pyridoxine	296 ± 4	74 ± 2	546 ± 55 (184)	255 ± 51 (345)	++++
Adenine	388 ± 12	83 ± 3	—[d]	—	—
All 6 supplements	182 ± 2	56 ± 4	270 ± 10 (148)	74 ± 1 (132)	+
5 supplements (no adenine)	195 ± 20	54 ± 2	235 ± 5 (121)	66 ± 4 (122)	+
5 supplements (no uracil)	398 ± 63	119 ± 3	>600 (>150)	394 ± 26 (331)	++++
4 supplements (no uracil or adenine)	235 ± 1	86 ± 2	263 ± 23 (112)	212 ± 13 (247)	++++

[a] Starter cultures were grown, washed, and resuspended as described for Table 1. A 0.1-ml volume of resuspended cells was inoculated into 10 ml of MMG with or without the following concentrations of supplements: uracil, 0.71 mM; methionine and isoleucine, 0.5 mM; thiamine, 0.03 mM; pyridoxine, 0.049 mM; and adenine, 0.4 mM (9). Cultures were grown with shaking at 37°C and monitored as described for Table 1. All values are expressed as the means ± standard errors of the means. $n = 2$ under all conditions except for when uracil, methionine, isoleucine, or adenine was added, in which cases $n = 3$.

[b] Percentages with respect to values for parent strain NU426 are indicated in parentheses.

[c] ++++, long (more than 50-μm) filaments predominant; +, mostly single cells, occasional short (<10-μm) filaments.

[d] —, cells in medium with adenine did not grow past double the initial Klett value.

was sufficient to restore nearly normal growth to *hisT*::Km^r knockout mutants. In addition, uracil dramatically reduced filament formation of *hisT*::Km^r mutants (Fig. 2c), although the resulting cells were about twice as long as the *hisT*$^+$ parent cells (Fig. 2a). Of the other five compounds, methionine noticeably reduced the lag time of *hisT* mutants but only slightly increased the doubling time and did not decrease filament formation (Table 2). The added requirements of the *hisT105* mutant reported by Bruni et al. (9) might have been a secondary effect due to partial uracil deprivation or to the accumulation of extragenic suppressors.

Thus, knockout mutations in *hisT* result in a uracil requirement that probably reflects a deficiency in the cellular UMP level. This metabolic defect may, in turn, lead to other secondary effects, such as dTTP deprivation, that interfere with replication and cell division. UMP shortage could result from defective attenuation of the *pyr* biosynthetic operons in *hisT*::Km^r mutants (22). For example, slower translation of the tandem Leu-Pro-Phe-Phe-Phe-Pro-Leu codons in the *pyrBI* leader peptide by pseudouridine-undermodified tRNA (20) should disrupt the synchronization between leader region transcription and translation, allow the terminator RNA structure to form frequently, and thereby reduce *pyrBI* operon expression, even though the cells are severely limited for UMP and UTP. Last, the uracil requirement of *hisT*::Km^r mutants may prove useful in genetic selections for increased UTP biosynthesis, since we noticed the occasional appearance of kanamycin-resistant, fast-growing pseudorevertants of *hisT*::Km^r mutants in MMG medium at 37°C (data not shown).

***hisT* gene expression is positively growth rate regulated and induced in early stationary phase.** Because *hisT*-mediated tRNA modification is essential for normal cell growth in minimal medium, we examined whether *hisT* expression is regulated by growth rate. Figure 3 shows that *hisT* is indeed positively growth rate regulated to about the same extent as reported for rRNA and tRNA genes (16) and *trmA*, which encodes tRNA(m^{5}U54) methyltransferase (14). Analysis of steady-state *hisT* transcript levels, corrected for variations in stable RNA content per genome equivalent at different growth rates (8), suggested that *hisT* growth rate regulation most likely occurs at the transcriptional level (data not shown). It remains to be determined whether increased *hisT* transcription at higher growth rates is from the primary (P_{pdxB}) or the strong internal (P_{int}) promoter of the complex *pdxB-hisT* operon (Fig. 1) (2, 4). P_{int}, like P_{trmA}, shares some features with rRNA operon promoters (2, 4, 14), although it is presently unclear in both cases whether these features play roles in positive growth rate regulation. Alternatively,

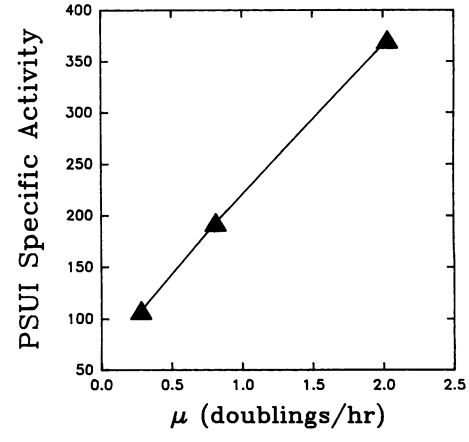

FIG. 3. Positive growth rate regulation of *hisT* gene expression in W3110 prototroph NU426. PSUI specific activities (expressed as counts per minute of ^{3}H released per minute per milligram of protein) in exponentially growing bacteria were measured as described previously (18). The different growth rates correspond to LBC, MMG plus 2 μg of thiamine per ml, and minimal (E) salts–0.4% (wt/vol) acetate–2 μg of thiamine per ml at 37°C. Control experiments ruled out enzyme instability or production of inhibitor as the cause of differences in PSUI specific activity at different growth rates (data not shown). Similar results were obtained for another prototrophic *E. coli* K-12 strain (data not shown).

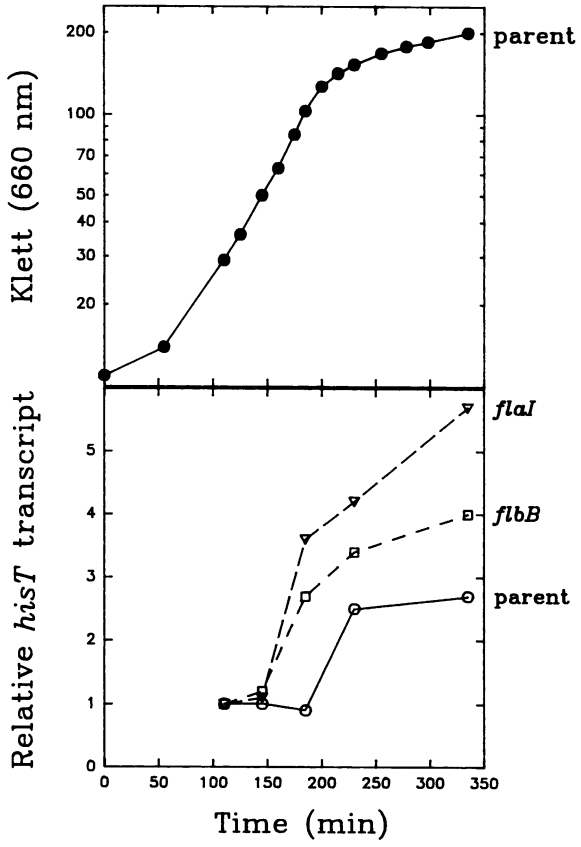

FIG. 4. *hisT* transcript levels in strains YK410 (*flbB*$^+$ *flaI*$^+$; circles), YK4131 (*flbB flaI*$^+$; squares), and YK4136 (*flbB*$^+$ *flaI*; triangles) (17) during the transition into stationary phase in LBC medium at 37°C. The upper and lower graphs show the growth curve for parent strain YK410 and the amount of *hisT* transcript relative to that in the exponential phase (≡1.0), respectively. *hisT* transcript levels were measured by RNase T_2 mapping as described previously (11). For each time point, the same amount of total cellular RNA was hybridized to an excess of a *hisT*-specific RNA probe. Full-length protected probe was resolved by gel electrophoresis and quantified by densitometry (11). Similar induction was observed for strain NU814 (*flbB*$^+$ *flaI*$^+$) (data not shown). When RNA was extracted from cells that were allowed to grow further into stationary phase, *hisT* transcript levels decreased to below the level detected in exponentially growing cells (data not shown).

positive growth rate regulation of *hisT* may involve changes in mRNA stability (13).

Finally, RNase T_2 transcript analysis performed as previously described (11) showed that the amount of *hisT* mRNA relative to the amount of total RNA was induced about three- to fivefold as cells entered stationary phase (Fig. 4). Induction of *hisT* transcription was not dependent on the *flaI* or *flbB* gene products, despite the presence of a FlaI-FlbB consensus-like regulatory sequence (6) immediately upstream from *hisT* (2).

Implications. The experiments in this report suggest that the regulation of key metabolic processes depends on the levels of tRNA modification. Loss of certain tRNA modifications can result in catastrophic defects (Fig. 2; Tables 1 and 2) that are much more severe than previously realized. The need to maintain tRNA modifications at appropriate cellular levels under different growth conditions implies that tRNA modification genes need to be strictly regulated. In the case of tRNA anticodon stem-and-loop pseudouridylation, *hisT* not only is a member of a complex operon (Fig. 1) but is regulated in at least two ways (Fig. 2 and 3). Future experiments will be aimed at learning the mechanisms responsible for *hisT* growth rate and stationary-phase regulation, especially in the context of the complex *pdxB-hisT* operon (Fig. 1).

We thank C. Gross, P. Matsumura, and C. Yanofsky for bacterial strains and H.-M. Lam, P. Matsumura, and B. B. Roa for helpful discussions.

This work was supported by Public Health Service grants GM37561 and GM43070 from the National Institute of General Medical Sciences to M.W.

REFERENCES

1. **Arena, F., G. Ciliberto, S. Ciampi, and R. Cortese.** 1978. Purification of pseudouridylate synthetase I from *Salmonella typhimurium*. Nucleic Acids Res. **5**:4523–4536.
2. **Arps, P. J., C. C. Marvel, B. C. Rubin, D. A. Tolan, E. E. Penhoet, and M. E. Winkler.** 1985. Structural features of the *hisT* operon of *Escherichia coli* K-12. Nucleic Acids Res. **13**:5297–5315.
3. **Arps, P. J., and M. E. Winkler.** 1987. An unusual genetic link between vitamin B_6 biosynthesis and tRNA pseudouridine modification in *Escherichia coli* K-12. J. Bacteriol. **169**:1071–1079.
4. **Arps, P. J., and M. E. Winkler.** 1987. Structural analysis of the *Escherichia coli* K-12 *hisT* operon by using a kanamycin resistance cassette. J. Bacteriol. **169**:1061–1070.
5. **Arps, P. J., and M. E. Winkler.** Unpublished result.
6. **Bartlett, D. H., B. B. Frantz, and P. Matsumura.** 1988. Flagellar transcriptional activators FlbB and FlaI: gene sequences and 5′ consensus sequences of operons under FlbB and FlaI control. J. Bacteriol. **170**:1575–1581.
7. **Björk, G. R.** 1987. Modification of stable RNA, p. 719–731. *In* F. C. Neidhardt, J. L. Ingraham, K. B. Low, B. Magasanik, M. Schaechter, and H. E. Umbarger (ed.), *Escherichia coli* and *Salmonella typhimurium*: cellular and molecular biology. American Society for Microbiology, Washington, D.C.
8. **Bremer, H., and P. P. Dennis.** 1987. Modulation of chemical composition and other parameters of the cell by growth rate, p. 1527–1542. *In* F. C. Neidhardt, J. L. Ingraham, K. B. Low, B. Magasanik, M. Schaechter, and H. E. Umbarger (ed.), *Escherichia coli* and *Salmonella typhimurium*: cellular and molecular biology. American Society for Microbiology, Washington, D.C.
9. **Bruni, C. B., V. Colantuoni, L. Sbordone, R. Cortese, and F. Blasi.** 1977. Biochemical and regulatory properties of *Escherichia coli* K-12 *hisT* mutants. J. Bacteriol. **130**:4–10.
10. **Chang, G. W., J. R. Roth, and B. N. Ames.** 1971. Histidine regulation in *Salmonella typhimurium*. VIII. Mutations of the *hisT* gene. J. Bacteriol. **108**:410–414.
11. **Connolly, D. M., and M. E. Winkler.** 1989. Genetic and physiological relationships among the *miaA* gene, 2-methylthio-N^6-(Δ^2-isopentenyl)-adenosine tRNA modification, and spontaneous mutagenesis in *Escherichia coli* K-12. J. Bacteriol. **171**: 3233–3246.
12. **Davis, R. W., D. Botstein, and J. R. Roth.** 1980. Advanced bacterial genetics. Cold Spring Harbor Laboratory, Cold Spring Harbor, N.Y.
13. **Emory, S. A., and J. G. Belasco.** 1990. The *ompA* 5′ untranslated RNA segment functions in *Escherichia coli* as a growth-rate-regulated mRNA stabilizer whose activity is unrelated to translational efficiency. J. Bacteriol. **172**:4472–4481.
14. **Gustafsson, C., P. H. R. Lindström, T. G. Hagervall, K. B. Esberg, and G. R. Björk.** 1991. The *trmA* promoter has regulatory features and sequence elements in common with the rRNA P1 promoter family of *Escherichia coli*. J. Bacteriol. **173**:1757–1764.
15. **Hiraga, S., H. Niki, T. Ogura, C. Ichinose, H. Mori, B. Ezaki, and A. Jaffé.** 1989. Chromosome partitioning in *Escherichia coli*: novel mutants producing anucleate cells. J. Bacteriol. **171**:1496–1505.

16. **Jinks-Robertson, S., and M. Nomura.** 1987. Ribosomes and tRNA, p. 1358–1385. *In* F. C. Neidhardt, J. L. Ingraham, K. B. Low, B. Magasanik, M. Schaechter, and H. E. Umbarger (ed.), *Escherichia coli* and *Salmonella typhimurium*: cellular and molecular biology. American Society for Microbiology, Washington, D.C.
17. **Komeda, Y., K. Kutsukake, and T. Iino.** 1980. Definition of additional flagellar genes (*fla*) of *Escherichia coli* K-12. Genetics **94**:277–290.
18. **Marvel, C. C., P. J. Arps, B. C. Rubin, H. O. Kammen, E. E. Penhoet, and M. E. Winkler.** 1985. *hisT* is part of a multigene operon in *Escherichia coli* K-12. J. Bacteriol. **161**:60–71.
19. **Murray, M. L., and P. E. Hartman.** 1972. Overproduction of *hisH* and *hisF* gene products leads to inhibition of cell division in *Salmonella*. Can. J. Microbiol. **18**:671–681.
20. **Palmer, D. T., P. H. Blum, and S. W. Artz.** 1983. Effects of the *hisT* mutation of *Salmonella typhimurium* on translation elongation rate. J. Bacteriol. **153**:357–363.
21. **Schoenlein, P. V., B. B. Roa, and M. E. Winkler.** 1989. Divergent transcription of *pdxB* and homology between the *pdxB* and *serA* gene products in *Escherichia coli* K-12. J. Bacteriol. **171**:6084–6092.
22. **Turnbough, C. L., K. L. Hicks, and J. P. Donahue.** 1983. Attentuation control of *pyrBI* operon expression in *Escherichia coli* K-12. Proc. Natl. Acad. Sci. USA **80**:368–372.